The pion-nucleon sigma term with $N_f = 2+1$ $O(a)$-improved Wilson fermions

A. Agadjanov,[a] **D. Djukanovic,**[b,c,*] **G. von Hippel,**[a] **H.B. Meyer,**[a,b,c] **K. Ottnad**[a] **and H. Wittig**[a,b,c]

[a] *PRISMA⁺ Cluster of Excellence & Institut für Kernphysik, Johannes Gutenberg-Universität Mainz, D-55099 Mainz, Germany*

[b] *Helmholtz Institute Mainz, Staudingerweg 18, D-55128 Mainz, Germany*

[c] *GSI Helmholtzzentrum für Schwerionenforschung, D-64291 Darmstadt*

E-mail: d.djukanovic@him.uni-mainz.de

We present an analysis of the pion-nucleon sigma term on the CLS ensembles with $N_f = 2+1$ flavors of $O(a)$-improved Wilson fermions. We perform a chiral interpolation based on ensembles with pion masses ranging from 130 MeV to roughly 350 MeV. The analysis covers four lattice spacings between $a \approx [0.05\,\text{fm}\dots0.09\,\text{fm}]$, allowing for an estimate of systematics associated with lattice artefacts.

The 39th International Symposium on Lattice Field Theory,
8th-13th August, 2022,
Rheinische Friedrich-Wilhelms-Universität Bonn, Bonn, Germany

---

[*]Speaker

1. Introduction

The pion-nucleon sigma term is defined as the matrix element of the scalar current

$$\sigma_{\pi N} = m_l \langle N | \bar{u}\, u + \bar{d}\, d | N \rangle \tag{1}$$

where u and d denote the up- and down-quark, m_l is the light quark mass, inserted between nucleon states $|N\rangle$. Alternatively the sigma term is accessible via the Feynman-Hellmann theorem [1, 2], that relates $\sigma_{\pi N}$ to derivatives of the nucleon mass with respect to the light quark masses $m_\ell = (m_u + m_d)/2$, i.e.

$$\sigma_{\pi N} = \frac{\partial}{\partial m_\ell} m_N. \tag{2}$$

The sigma term is of particular phenomenological interest, as it proves vital in constraining beyond standard model physics. More specifically, a promising class of dark matter candidates, the so-called weakly interacting massive particles, may leave an imprint in scattering with ordinary nuclear matter via scalar interactions. The contribution of the spin-independent cross section to the rate of the WIMP-nucleus scattering is enhanced by the number of nuclei within the nucleus [3]. Given the pion-nucleon sigma term one thus may infer bounds on the masses of WIMPs via direct detection experiments measuring the recoil energy of heavy nuclei scattered on WIMPs, e.g. Xenon [4] or CDMS [5].

Despite the lack of a scalar probe for experiments, there still is a connection to an experimentally accessible quantity, i.e. pion nucleon scattering lengths. This connection is established via the Cheng-Dashen low energy theorem [6], that relates the scattering amplitudes from pion-nucleon scattering at subthreshold kinematics, to the scalar form factor. In the framework of Roy-Steiner equations the following value for the pion-nucleon sigma term has been obtained [7]

$$\sigma_{\pi N} = (59.1 \pm 3.5)\,\text{MeV}. \tag{3}$$

However, comparing this phenomenological value to recent determinations from the lattice [8–13], a slight tension emerges, where lattice extractions tend to smaller values. Most recently, in Ref. [9] it was argued that this discrepancy might be alleviated with a careful treatment of excited states in the direct determination.

In this proceedings contribution, we report on progress in extracting the pion-nucleon sigma term on CLS ensembles with $N_f = 2 + 1$ $O(a)$ improved Wilson fermions [14]. We focus on the direct extraction, calculating the matrix element of Eq. (1).

2. Lattice Methodology

The Wick contractions for the scalar matrix element of Eq. (1) generate connected and quark-disconnected contributions. For the connected contributions we apply the standard methods, as described in [15], where sequential propagators are calculated in a fixed-sink setup. We calculate
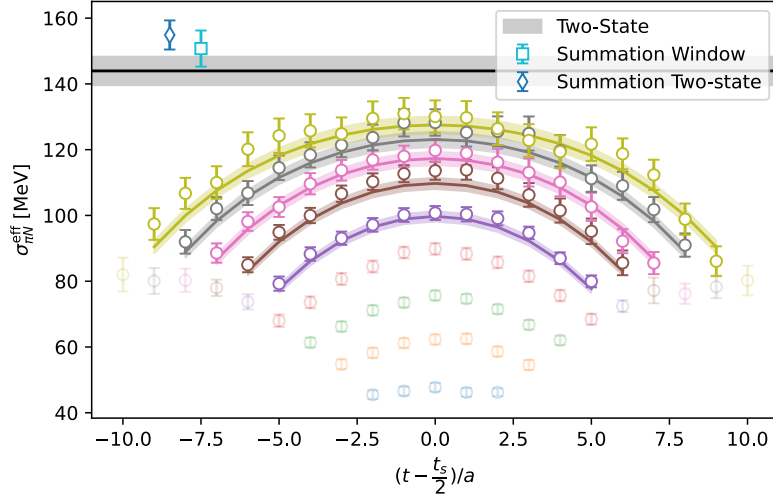
Figure 1: Comparison of the extracted values for the summation window, summation two-state, and explicit two-state analysis on ensemble N451. The data points show the effective form factor for all insertion times of the current between source and sink. The colored bands are the result of the two-state fit using Eq. (13), while the grey band corresponds to the extracted ground-state matrix element.

the two-point function and the three-point function of the scalar current

$$C_2(t, \vec{p}) = \Gamma_{\alpha\beta} \sum_{\vec{x}} e^{-i\vec{p}\vec{x}} \langle \Psi_\beta(\vec{x}, t) \bar{\Psi}_\alpha(0) \rangle, \tag{4}$$

$$C_3^q(t, t_s, \vec{q}) = \Gamma_{\alpha\beta} \sum_{\vec{x}, \vec{y}} e^{i\vec{q}\vec{y}} \langle \Psi_\beta(\vec{x}, t_s) O^q(\vec{y}, t) \bar{\Psi}_\alpha(0) \rangle, \tag{5}$$

where the nucleon interpolating operator is given by

$$\Psi_\alpha(x) = \epsilon_{abc} \left(\tilde{u}_a^T(x) C \gamma_5 \tilde{d}_b(x) \right) \tilde{u}_{c,\alpha}(x), \tag{6}$$

and the operator of the local scalar current for a quark of flavor q reads

$$O^q(x) = \bar{q}(x) \mathbb{I} q(x). \tag{7}$$

The quark fields are Gaussian-smeared [16]

$$\tilde{q} = (1 + \kappa_G \Delta)^{N_G} q, \qquad q = u, d, \tag{8}$$

using spatially APE-smeared gauge links in the covariant Laplacian Δ [17].

For the disconnected part we use a variation of the frequency splitting method [18], combining the one-end-trick [19], generalized hopping parameter expansion [20] and hierarchical probing [21] (for more details see Ref. [22]) to estimate the quark loops. The disconnected three-point function is given in terms of the quark loop and the nucleon two-point function

$$C_3^{q,\text{disc}}(t, t_s; \vec{0}) = \langle L^q(\vec{0}, t) \hat{C}_2(t_s, \vec{p} = \vec{0}) \rangle, \tag{9}$$
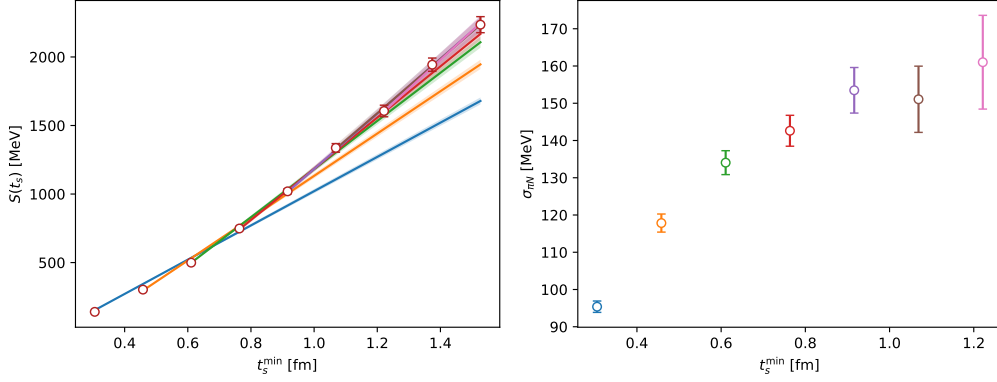
Figure 2: Left: Linear fits to the summed correlator (data points) on ensemble N451, i.e. Eq. (12) with $c_{10} = c_{11} = 0$, for different starting source-sink separations. The right panel shows the corresponding values for $\sigma_{\pi N}$ for the different fits, where the color of the data points match the color of the corresponding fit in the left plot.

where L^q denotes the trace over quark loops of flavor q. For the forward matrix element, the vacuum expectation of the loop and the two-point functions need to be subtracted. We reduce the variance for two- and three-point functions applying the truncated solver method with bias correction [23–25]. For details on the setup and the ensembles used see Ref. [26].

The scalar form factor may be extracted as the ratio of three- and two-point functions

$$\text{Re} \frac{C_3^q(t, t_s)}{C_2(t, t_s)} \xrightarrow{t,(t_s-t)\gg 0} G_S^q, \tag{10}$$

in the asymptotic limit of large time separations. The pion-nucleon sigma term is a linear combination of the asymptotic ratios and light quark masses. It is convenient to build an effective form factor, the asymptotic limit of which coincides with $\sigma_{\pi N}$. In Fig. 1, we show such an effective form factor for the ensemble N451. In the region of large time separation to either source or sink one expects a plateau, where the ground state dominates. The lack of a clear plateau region, i.e. the curvature in Fig. 1, already hints at sizeable effects due to excited states in this quantity.

3. Excited States

As a consequence of the unfavorable signal-to-noise ratio for matrix elements of baryonic operators [27], most calculations in the baryon sector suffer from contamination due to excited states (see [28] and references therein). We therefore have to include effects of excited states into the analysis of the correlators. In order to assess the remnant excited-state contribution, we compare the extraction based directly on the ratio of correlators and alternatively from the summed correlator. The latter is less sensitive to contributions from excited states, as these are parametrically more suppressed [29–32]. We define the summed correlator of the effective form factor

$$S(t_s) = \sum_{t=a}^{t_s-a} G_S^{\text{eff}}(t, t_s). \tag{11}$$

4
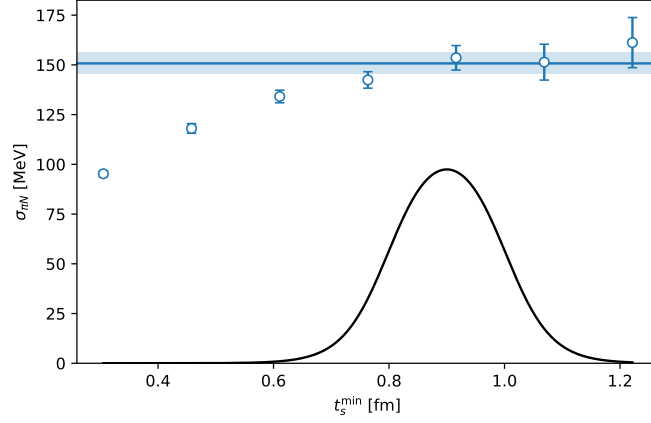
Figure 3: Estimates for the pion-nucleon sigma term extracted via the summation method, plotted as a function of the minimum source-sink separation t_s^{min}. The blue shaded area corresponds to the window average using the weights of Eq. (14) for the summation extraction at different starting time slices t_s^{min} (blue data points) for ensemble N451. The black line shows the profile of the weights for the parameters t_s^{min}.

Including one excited state in the summed correlator, its asymptotic behavior reads

$$S(t_s) = (G_S + c_{11}e^{-\Delta t_s})(t_s - 1) + 2c_{10}e^{-\Delta t_s/2}\mathrm{csch}\frac{\Delta}{2}\sinh\frac{1}{2}(t_s - 1) + \ldots, \tag{12}$$

where Δ denotes the energy gap between ground and first excited state, and c_{10}, c_{11} are the overlaps of the scalar current with ground-excited, and excited-excited states, respectively. Alternatively one may directly fit the effective form factor using an explicit two-state ansatz

$$G_S^{\mathrm{eff}} = G_S + c_{10}e^{-\Delta t} + c_{10}e^{-\Delta(t_s - t)} + c_{11}e^{-\Delta t_s}. \tag{13}$$

We extend the available source-sink separations to include smaller values, down to $t_s = 4$ in lattice units, see Ref. [26]. This enables us to monitor the stability of the extraction of the matrix element based on a linear fit to the summed correlator, i.e. assuming ground state dominance.

In Fig. 2 we show the linear fit of Eq. (12) as a function of the starting time slice t_s^{min} for ensemble N451. The corresponding values for the sigma-term are shown in the right panel, where the onset of a plateau in the extraction is visible starting around 0.9 fm. We see that for very small t_s^{min} the extraction is still biased by the influence from excited states, while for large t_s^{min} the error increases. With this in mind, instead of choosing one particular t_s^{min} to quote a final value for the summation method, we perform averages based on weights (see Ref. [26])

$$w_i = \frac{1}{2}\tanh\frac{t_s - t_{\mathrm{lo}}}{\delta t} - \frac{1}{2}\tanh\frac{t_s - t_{\mathrm{up}}}{\delta t}. \tag{14}$$

These weights effectively define a window that suppresses unreliable estimates at very early starting times and, at the same time, reduces the influence of the noisy estimates at larger t_s^{min}. The parameters for the window are fixed in physical units and applied uniformly to all ensembles. We find

$$t_{\mathrm{lo}} = 0.8 \text{ fm}, \quad t_{\mathrm{up}} = 1.0 \text{ fm}, \quad \text{and} \quad \delta t = 0.08 \text{ fm} \tag{15}$$
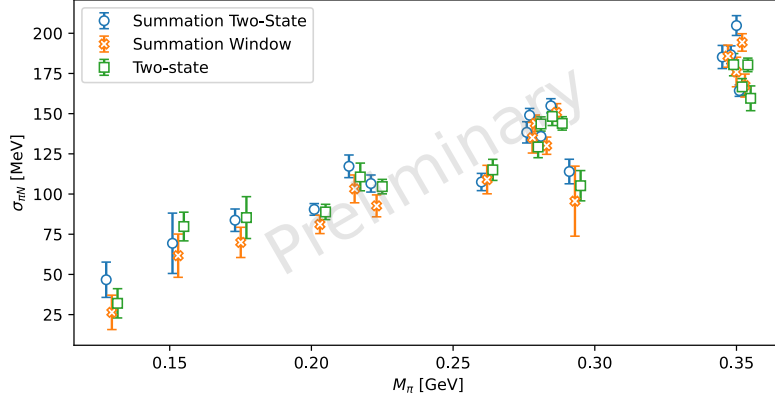
Figure 4: Comparison of the extracted values for $\sigma_{\pi N}$ on all ensembles using the window average of the summed correlator (orange crosses), the two-state ansatz for the summed correlator (blue circle) and the direct two-state ansatz (green squares).

leads to a stable set of estimates for the ground state matrix element. In addition, we fit the summed correlator using the ansatz of Eq. (12), i.e. including excited states. However, the term corresponding to the excited-excited contribution c_{11}, as well as the energy gap between ground and first excited state Δ are not well constrained. We therefore choose a simplified ansatz, removing c_{11} and, to stabilize the fits, apply Gaussian priors for the energy gap Δ, with a central value corresponding to two non-interacting pions on the respective ensemble with a width of 5 %. The same caveats apply to the direct two-state fit ansatz of Eq. (13). In Fig. 4 we compare the different extractions, and observe agreement within 2 standard deviations.

4. Chiral and Continuum Extrapolation

The chiral expansion of the nucleon mass is known to sixth order in the chiral counting [33]. However, given the rapid growth in the number of coupling constants, we restrict ourselves to the SU(2) expression at fourth chiral order, which, amended with terms parametrizing lattice spacing dependence and finite volume corrections, reads

$$\sigma_{\pi N} = (k_1 + k_a a)M_\pi^2 + k_2 M_\pi^3 + 2k_3 M_\pi^4 \log \frac{M_\pi}{\mu} + k_4 M_\pi^4 + k_L M_\pi^2 \left[\frac{1}{L} - \frac{M_\pi}{2} \right] e^{-M_\pi L}. \quad (16)$$

The functional form of the finite volume corrections is taken from [34]. The coefficients k_1, k_2 and k_3 depend on known low-energy constants (LECs), while k_4 receives contributions from a less well known fourth order LEC and contributions from the mesonic Lagrangian at fourth order. Leaving all couplings free leads to unstable fits, especially after applying cuts in the pion mass. We may stabilize the fits by either dropping terms, noting that otherwise large cancellation happen between fourth order terms, or fixing some of the coefficients to the values known from ChPT. Instead of
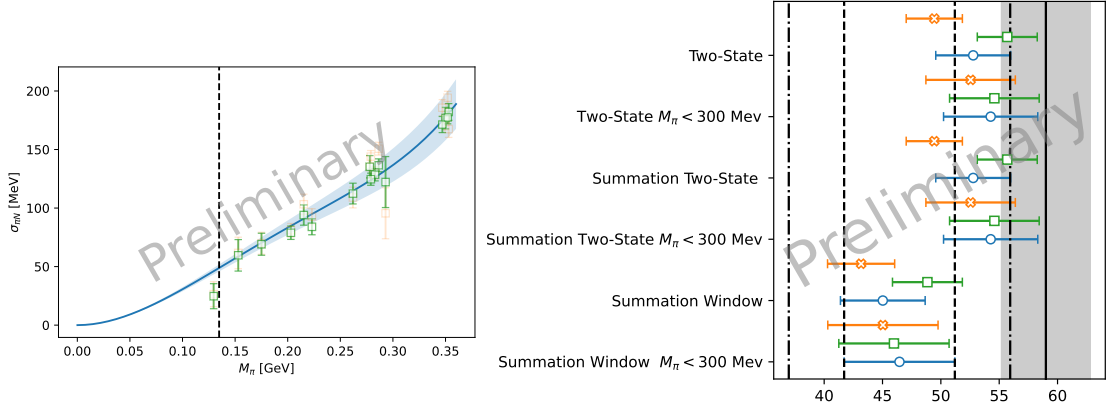
Figure 5: Left: Fit using the full form of Eq. (16), without a cut in the pion mass on the window averaged summation data points in green/light orange, with/without corrections due to lattice spacing and finite volume applied. Right: Compilation of results obtained using the three variations of the ChPT expressions, i.e. blue points, green square and orange cross, correspond to third order fits, including the full form, dropping the chiral log, respectively, on all data sets, and with pion mass cuts as indicated in the label. The grey band corresponds to the dispersive analysis of Ref. [7].

completely fixing the values we choose to apply Gaussian priors on the LECs, i.e.

$$k_1 = -4c_1 = (4.44 \pm 0.12) \text{ GeV}^{-1}, \tag{17}$$

$$k_2 = -\frac{9g_A^2}{64\pi F_\pi^2} = (-8.52 \pm 0.04) \text{ GeV}^{-2}, \tag{18}$$

$$k_3 = -\frac{3}{32\pi^2 F_\pi^2}\left(\frac{g_A^2}{m_n} - 8c_1 + c_2 + 4c_3\right) - \frac{c_1}{8\pi^2 F_\pi^2} = (-11.38 \pm 0.35) \text{ GeV}^{-3}, \tag{19}$$

where the values for the LECs are taken from [35]. The left panel of Fig. 5 shows one particular fit, using the full form of Eq. (16) on summation window averaged data on all ensembles. We further analyze variations of Eq. (16) in order to assess the relevance of individual terms to the final result. In the right panel of Fig. 5 we compare results from three types of ChPT ansätze: (1) using ChPT including terms up to third order, (2) dropping the chiral log, i.e. k3 = 0 and (3) the full expression of Eq. (16). Each ansatz is applied to the different data sets as explained in Sec. 3, either with a cut of 300 MeV in the pion mass, or over the full pion mass range. In general the variations for the fit functions agree quite well within each set, while for the data sets with an explicit two-state ansatz including priors for the energy gap, a systematic shift towards larger values of $\sigma_{\pi N}$ is visible. However, the errors are still quite large and all extractions agree within two standard deviations. Nevertheless it is evident that excited states play an important role for the scalar matrix element.

We intend to further increase statistics, especially for the disconnected part, and perform fits based on SU(3) ChPT expressions, in order to have a handle on the strange sigma term σ_s. Furthermore, including constraints from the nucleon mass dependence might prove helpful to further constrain the sigma terms.

5. Acknowledgments

References

[1] R.P. Feynman, *Forces in Molecules*, *Phys. Rev.* **56** (1939) 340.

[2] H. Hellmann, *Zur Rolle der kinetischen Elektronenenergie für die zwischenatomaren Kräfte*, *Zeitschrift für Physik* **85** (1933) 180.

[3] J.R. Ellis, K.A. Olive and C. Savage, *Hadronic Uncertainties in the Elastic Scattering of Supersymmetric Dark Matter*, *Phys. Rev. D* **77** (2008) 065026 [0801.3656].

[4] XENON collaboration, *Dark Matter Search Results from a One Ton-Year Exposure of XENON1T*, *Phys. Rev. Lett.* **121** (2018) 111302 [1805.12562].

[5] CDMS-II collaboration, *Results from a Low-Energy Analysis of the CDMS II Germanium Data*, *Phys. Rev. Lett.* **106** (2011) 131302 [1011.2482].

[6] T.P. Cheng and R.F. Dashen, *Is SU(2) x SU(2) a better symmetry than SU(3)?*, *Phys. Rev. Lett.* **26** (1971) 594.

[7] M. Hoferichter, J. Ruiz de Elvira, B. Kubis and U.-G. Meißner, *High-Precision Determination of the Pion-Nucleon σ Term from Roy-Steiner Equations*, *Phys. Rev. Lett.* **115** (2015) 092301 [1506.04142].

[8] C. Alexandrou, S. Bacchio, M. Constantinou, J. Finkenrath, K. Hadjiyiannakou, K. Jansen et al., *Nucleon axial, tensor, and scalar charges and σ-terms in lattice QCD*, *Phys. Rev. D* **102** (2020) 054517 [1909.00485].

[9] R. Gupta, S. Park, M. Hoferichter, E. Mereghetti, B. Yoon and T. Bhattacharya, *Pion–Nucleon Sigma Term from Lattice QCD*, *Phys. Rev. Lett.* **127** (2021) 242002 [2105.12095].

[10] xQCD collaboration, *πN and strangeness sigma terms at the physical point with chiral fermions*, *Phys. Rev. D* **94** (2016) 054503 [1511.09089].

[11] JLQCD collaboration, *Nucleon charges with dynamical overlap fermions*, *Phys. Rev. D* **98** (2018) 054516 [1805.10507].

[12] S. Borsanyi, Z. Fodor, C. Hoelbling, L. Lellouch, K.K. Szabo, C. Torrero et al., *Ab-initio calculation of the proton and the neutron's scalar couplings for new physics searches*, 2007.03319.

[13] RQCD collaboration, *Direct determinations of the nucleon and pion σ terms at nearly physical quark masses*, *Phys. Rev. D* **93** (2016) 094504 [1603.00827].

[14] M. Bruno et al., *Simulation of QCD with $N_f = 2 + 1$ flavors of non-perturbatively improved Wilson fermions*, *JHEP* **02** (2015) 043 [1411.3982].

[15] D. Djukanovic, T. Harris, G. von Hippel, P.M. Junnarkar, H.B. Meyer, D. Mohler et al., *Isovector electromagnetic form factors of the nucleon from lattice QCD and the proton radius puzzle*, *Phys. Rev. D* **103** (2021) 094522 [2102.07460].

[16] S. Güsken, U. Löw, K.H. Mütter, R. Sommer, A. Patel and K. Schilling, *Nonsinglet Axial Vector Couplings of the Baryon Octet in Lattice QCD*, *Phys. Lett. B* **227** (1989) 266.

[17] APE collaboration, *Glueball Masses and String Tension in Lattice QCD*, *Phys. Lett. B* **192** (1987) 163.

[18] L. Giusti, T. Harris, A. Nada and S. Schaefer, *Frequency-splitting estimators of single-propagator traces*, *Eur. Phys. J. C* **79** (2019) 586 [1903.10447].

[19] UKQCD collaboration, *Decay width of light quark hybrid meson from the lattice*, *Phys. Rev. D* **73** (2006) 074506 [hep-lat/0603007].

[20] V. Gülpers, G. von Hippel and H. Wittig, *Scalar pion form factor in two-flavor lattice QCD*, *Phys. Rev. D* **89** (2014) 094503 [1309.2104].

[21] A. Stathopoulos, J. Laeuchli and K. Orginos, *Hierarchical probing for estimating the trace of the matrix inverse on toroidal lattices*, 1302.4018.

[22] T. San José, H. Wittig, M. Cè, A. Gérardin, G. von Hippel, H.B. Meyer et al., *The hadronic running of the electromagnetic coupling and the electroweak mixing angle from lattice QCD*, *JHEP* **08** (2022) 220 [2203.08676].

[23] G.S. Bali, S. Collins and A. Schafer, *Effective noise reduction techniques for disconnected loops in Lattice QCD*, *Comput. Phys. Commun.* **181** (2010) 1570 [0910.3970].

[24] T. Blum, T. Izubuchi and E. Shintani, *New class of variance-reduction techniques using lattice symmetries*, *Phys. Rev. D* **88** (2013) 094503 [1208.4349].

[25] E. Shintani, R. Arthur, T. Blum, T. Izubuchi, C. Jung and C. Lehner, *Covariant approximation averaging*, *Phys. Rev. D* **91** (2015) 114511 [1402.0244].

[26] D. Djukanovic, G. von Hippel, J. Koponen, H.B. Meyer, K. Ottnad, T. Schulz et al., *Isovector axial form factor of the nucleon from lattice QCD*, *Phys. Rev. D* **106** (2022) 074503 [2207.03440].

[27] G.P. Lepage, *The Analysis of Algorithms for Lattice Field Theory*, in *Theoretical Advanced Study Institute in Elementary Particle Physics*, 6, 1989.

[28] D. Djukanovic, *Recent progress on nucleon form factors*, *PoS* **LATTICE2021** (2022) 009 [2112.00128].

[29] L. Maiani, G. Martinelli, M.L. Paciello and B. Taglienti, *Scalar Densities and Baryon Mass Differences in Lattice QCD With Wilson Fermions*, *Nucl. Phys. B* **293** (1987) 420.

[30] S.J. Dong, K.F. Liu and A.G. Williams, *Lattice calculation of the strangeness magnetic moment of the nucleon*, *Phys. Rev. D* **58** (1998) 074504 [hep-ph/9712483].

[31] S. Capitani, M. Della Morte, G. von Hippel, B. Jäger, A. Jüttner, B. Knippschild et al., *The nucleon axial charge from lattice QCD with controlled errors*, *Phys. Rev. D* **86** (2012) 074502 [1205.0180].

[32] J.R. Green, J.W. Negele, A.V. Pochinsky, S.N. Syritsyn, M. Engelhardt and S. Krieg, *Nucleon electromagnetic form factors from lattice QCD using a nearly physical pion mass*, *Phys. Rev. D* **90** (2014) 074507 [1404.4029].

[33] M.R. Schindler, D. Djukanovic, J. Gegelia and S. Scherer, *Chiral expansion of the nucleon mass to order(q**6)*, *Phys. Lett. B* **649** (2007) 390 [hep-ph/0612164].

[34] S.R. Beane, *Nucleon masses and magnetic moments in a finite volume*, *Phys. Rev. D* **70** (2004) 034507 [hep-lat/0403015].

[35] M. Hoferichter, J. Ruiz de Elvira, B. Kubis and U.-G. Meißner, *Roy–Steiner-equation analysis of pion–nucleon scattering*, *Phys. Rept.* **625** (2016) 1 [1510.06039].

[36] SCIDAC, LHPC, UKQCD collaboration, *The Chroma software system for lattice QCD*, *Nucl. Phys. B Proc. Suppl.* **140** (2005) 832 [hep-lat/0409003].

[37] M. Lüscher and S. Schaefer, *Lattice QCD with open boundary conditions and twisted-mass reweighting*, *Comput. Phys. Commun.* **184** (2013) 519 [1206.2809].

[38] D. Djukanovic, *Quark Contraction Tool — QCT*, *Comput. Phys. Commun.* **247** (2020) 106950 [1603.01576].